EXTENDING μ P: SPECTRAL CONDITIONS FOR FEATURE LEARNING ACROSS OPTIMIZERS

Anonymous authors

Paper under double-blind review

ABSTRACT

Several variations of adaptive first-order and second-order methods have been proposed to accelerate and scale the training of large language models. The performance of optimization routines is highly sensitive to the choice of hyperparameters (HPs), which are computationally expensive to tune for large-scale models. Maximal update parameterization (μP) is a set of scaling rules which aims to make the optimal HPs independent of the model size, thereby allowing the HPs tuned on a smaller (computationally cheaper) model to be transferred to train a larger, target model. Despite promising results for SGD and Adam, deriving μP for other optimizers is challenging because the underlying tensor programming approach is difficult to grasp. Building on recent work that introduced spectral conditions as an alternative to tensor programs, we propose a novel framework to derive μP for a broader class of optimizers, including AdamW, ADOPT, LAMB, Sophia and Shampoo. We validate our derivations on different benchmark models and demonstrate zero-shot learning rate transfer across increasing model width for the above optimizers. Further, we provide empirical insights into depth-scaling parameterization for these optimizers.

1 Introduction

Large language models (LLMs) have achieved remarkable progress in generative AI, yet their performance and reproducibility depend on many interacting factors. A key aspect of training LLMs is the optimization routine, which can become unstable as models grow in size and complexity. To improve stability and efficiency, several modifications to existing optimizers have been proposed. For example, LAMB (You et al. (2019)) proposes a layer-wise adaptive optimization routine to reduce the computational time required for training deep neural networks over large mini-batches, while Sophia (Liu et al. (2023)) is a light-weight second-order method which achieves faster convergence than Adam while being more robust to non-convex landscapes. Muon is another recent optimizer designed explicitly for scaling with model size (Jordan et al. (2024); Liu et al. (2025)).

Although these recent algorithms demonstrate strong performance, the computational overhead of hyperparameter (HP) tuning poses a fundamental scalability bottleneck for training LLMs. To address this challenge, practitioners have heuristically tuned HPs on smaller models to guide the search for optimal configurations in larger models. Recent works (Yang et al. (2021); Yang & Hu (2020)) have formalized this approach by proposing a zero-shot HP transfer algorithm based on maximal update parameterization (μ P), which stabilizes feature learning across different model widths. μ P is implemented by carefully scaling the weights and HPs proportional to the model width, with scaling factors tailored to the specific architecture and optimization algorithm. Under μ P, feature learning is stable throughout the training process and HPs are stable across increasing model width.

For the above reasons, several recent works have derived and incorporated μP for different models (Zheng et al. (2025); Thérien et al.) and optimization algorithms (Blake et al. (2025b); Ishikawa & Karakida). Fig. 1 demonstrates the increased training stability and predictability after μP is incorporated in Muon. Fig. 1 (left) shows that the relative mean of different feature vectors remains stable with increasing model width, thereby ensuring maximal (weights not decreasing to 0) and stable (weights not diverging) feature learning under μP . Fig. 1 (middle) demonstrates zero-shot learning rate transfer across increasing model width where the best validation loss is obtained at learning rate 0.1 for all model widths. Finally, Fig. 1 (right) demonstrates the "wider is always better" property where the training loss improves consistently with increasing model width under μP .

While μP delivers strong results, it is tedious to implement in existing large codebases and difficult to understand in practice. To address this, authors in Yang et al. (2023a) proposed simpler spectral scaling conditions on the weight matrices that lead to the same width-independent and maximal feature learning properties of μP . This work focuses on using the more tractable spectral conditions to derive μP for a wide range of optimizers. Despite being more intuitive, using spectral conditions to derive μP is not trivial and the analysis for each adaptive optimizer is different and requires a careful study of the order-of-magnitude of the coefficient terms that scale the gradients.

Our contributions are threefold: (1) we derive μP for adaptive first and second-order optimizers (AdamW, ADOPT, LAMB, Sophia, Shampoo) via a novel spectral scaling approach; (2) we demonstrate zero-shot HP transfer (specifically of the optimal learning rate) across model width on benchmark LLMs (NanoGPT (Karpathy (2022)); Llama2 (Touvron et al. (2023))); and (3) we provide an empirical study of zero-shot HP transfer across model depth for these optimizers.

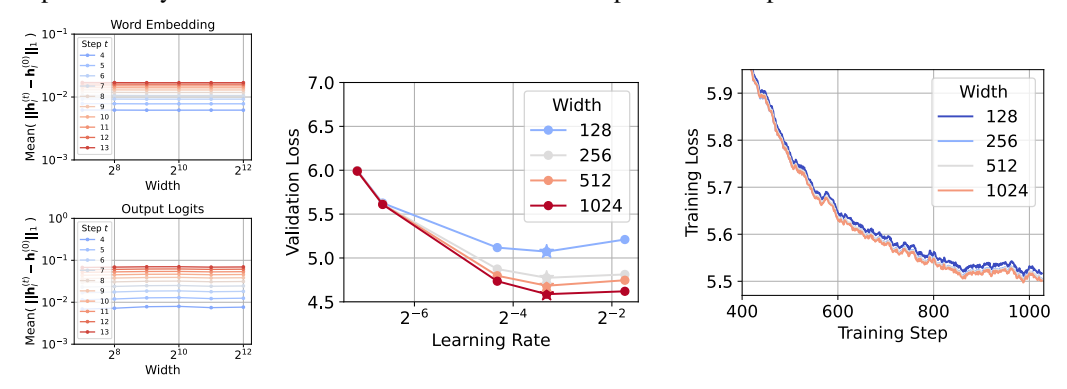


Figure 1: μ P for Muon (trained on Llama2) - Coordinate check plots for the word embedding and output logits layers (left); Zero-shot learning rate transfer across increasing model width (middle); Decreasing training loss with increasing model width (right).

2 Preliminaries

The l^p -norm of a vector $\mathbf{x} \in \mathbb{R}^n$ is defined as $||\mathbf{x}||_p := \left(\sum_{i=1}^n |x_i|^p\right)^{1/p}$. For a matrix $\mathbf{A} \in \mathbb{R}^{n \times n}$, $\mathbf{A}^\alpha = \sum_i \lambda_{e_i}^\alpha \mathbf{u}_i \mathbf{u}_i^\mathrm{T}$ where $(\lambda_{e_i}, \mathbf{u}_i)$ are the i-th eigen pair. The spectral norm of a matrix $\mathbf{A} \in \mathbb{R}^{m \times n}$ is defined as $||\mathbf{A}||_* := \max_{\mathbf{x} \in \mathbb{R}^n \setminus \{\mathbf{0}\}} \frac{||\mathbf{A}\mathbf{x}||_2}{||\mathbf{x}||_2}$, and the Frobenius norm is defined as $||\mathbf{A}||_F := \sqrt{\sum_{i=1}^m \sum_{j=1}^n |\mathbf{A}_{i,j}|^2}$ (Strang (2012); Meyer (2023)). If r denotes the rank of matrix \mathbf{A} , then $||\mathbf{A}||_* \le ||\mathbf{A}||_F \le \sqrt{r}||\mathbf{A}||_*$. If a matrix $\mathbf{A} \in \mathbb{R}^{m \times n}$ can be written as an outer product of some vectors $\mathbf{u} \in \mathbb{R}^m$ and $\mathbf{v} \in \mathbb{R}^n$, that is, $\mathbf{A} = \mathbf{u}\mathbf{v}^\mathrm{T}$ then matrix \mathbf{A} is a rank one matrix and

$$||\mathbf{A}||_* = ||\mathbf{A}||_F = ||\mathbf{u}||_2 \cdot ||\mathbf{v}||_2.$$
 (1)

For any symmetric matrix, the spectral norm is equal to the absolute value of the maximum eigen value. Therefore, for $p \in \mathbb{R}$, for a symmetric rank one matrix $\mathbf{A} = \mathbf{u}\mathbf{u}^T \in \mathbb{R}^{n \times n}$,

$$||\mathbf{A}^p||_* = ||\mathbf{A}||_*^p. \tag{2}$$

A sequence of random vectors $\{\mathbf{x}_i \in \mathbb{R}^n\}_{i=1}^\infty$ is said to have $\Theta(n^\alpha)$ -sized coordinates if there exists constants A,B such that $An^\alpha \leq \sqrt{\frac{||\mathbf{x}_i||_2^2}{n}} \leq Bn^\alpha$ for all i, and for sufficiently large n.

3 BACKGROUND

In Sections 3 and 4, μ P is derived for a linear MLP trained with a batch size of 1, similar to the model used in Yang et al. (2023a). Let us consider an MLP with L layers. Let $\mathbf{x} \in \mathbb{R}^{n_0}$ denote the input vector and $\mathbf{W}_l \in \mathbb{R}^{n_l \times n_{l-1}}$ denote the weight matrix for the l-th layer of the model. Then the feature vector $\mathbf{h}_l \in \mathbb{R}^{n_l}$ for the input \mathbf{x} is given as

$$\mathbf{h}_{l}(\mathbf{x}) = \mathbf{W}_{l} \mathbf{h}_{l-1}(\mathbf{x}), \qquad \forall l = 1, 2, \dots, L$$
(3)

where $\mathbf{h}_0(\mathbf{x}) = \mathbf{x}$. Let $\mathcal{L} = g(\mathbf{h}_L(\mathbf{x}), \mathbf{y})$ denote the loss, where $g : \mathbb{R}^{n_0} \times \mathbb{R}^{n_L} \to \mathbb{R}$ is a loss function, $\mathbf{y} \in \mathbb{R}^{n_L}$ is the target vector corresponding to the input \mathbf{x} and $\mathbf{h}_L(\mathbf{x}) \in \mathbb{R}^{n_L}$ is the output

 vector returned by the MLP. After one step of training, the change in the weight matrices is typically a function, $\Psi(\cdot)$, of the history of the gradients. Then, the change in weights from time instant t to t+1 can be written using the following generic update rule,

$$\mathbf{W}_{l}^{(t+1)} = \mathbf{W}_{l}^{(t)} - \eta^{(t)} \Psi(\{\nabla_{\mathbf{W}_{l}^{(i)}} \mathcal{L}\}_{i=1}^{t})$$
(4)

where $\eta^{(t)}$ is the learning rate at time instant t. We specify the forms of $\Psi(\cdot)$ for different optimizers in Table 1. To reduce cumbersome notation, we omit time indices in the remaining sections unless their inclusion is necessary for clarity. This will not affect the derivation of μP as it is sufficient to analyze a single step of rule (4) to determine the correct scaling laws (Yang et al. (2021); Blake et al. (2025a)). Using eqs. (3) and (4) the change in weights and feature vectors for any layer l, after one training step can be written as

$$\Delta \mathbf{W}_l = -\eta \Psi(\{\nabla_{\mathbf{W}_l} \mathcal{L}\})$$
 and $\Delta \mathbf{h}_l(\mathbf{x}) = \Delta \mathbf{W}_l \mathbf{h}_{l-1}(\mathbf{x}) + \Delta \mathbf{W}_l \Delta \mathbf{h}_{l-1}(\mathbf{x}) + \mathbf{W}_l \Delta \mathbf{h}_{l-1}(\mathbf{x}).$

Optimizer	$\Psi(\cdot)$
AdamW / ADOPT	$rac{\hat{\mathbf{m}}^{(t)}}{\sqrt{\hat{\mathbf{v}}^{(t)}} + \epsilon} + \lambda \mathbf{W}_l^{(t)}$
Sophia	$\operatorname{clip}\!\left(\frac{\mathbf{m}^{(t)}}{\max\{\gamma\mathbf{h}^{(t)},\epsilon\}},1\right) + \lambda\mathbf{W}_l^{(t)}$
LAMB	$\frac{\hat{\mathbf{m}}^{(t)}}{\sqrt{\hat{\mathbf{v}}^{(t)}} + \epsilon} + \lambda \mathbf{W}_{l}^{(t)}$ $\operatorname{clip}\left(\frac{\mathbf{m}^{(t)}}{\max\{\gamma \mathbf{h}^{(t)}, \epsilon\}}, 1\right) + \lambda \mathbf{W}_{l}^{(t)}$ $\frac{\phi(\mathbf{W}_{l}^{(t)} _{\mathrm{F}})}{ \mathbf{r}_{l}^{(t)} + \lambda \mathbf{W}_{l}^{(t)} _{\mathrm{F}}} \left(\mathbf{r}_{l}^{(t)} + \lambda \mathbf{W}_{l}^{(t)}\right)$
Shampoo	$(\mathbf{L}^{(t)})^{-1/4} \stackrel{\iota}{ abla}_{\mathbf{W}_l^{(t)}} \mathcal{L} (\mathbf{R}^{(t)})^{-1/4}$

Table 1: Values of $\Psi(\cdot)$ for different optimizers. Auxiliary variables are defined in Section 4.

3.1 MAXIMAL UPDATE PARAMETRIZATION (μP)

Authors in (Yang & Hu (2020); Yang et al. (2021)) proposed μP to ensure that overparameterized models do not learn trivial features, or that the feature values do not blow up with increasing model width. In practice, μP is implemented via the abc-parameterization (Yang & Hu (2020)) which ensures that the MLP weights, their initial variance and the learning rate are appropriately scaled with respect to the width of the model. In Yang & Hu (2020), the abc-parameterization was introduced for MLPs where the hidden layers have the same width, that is, $n_{l-1} = n_l = n$ for $l = 2, \ldots, L-1$. For simplicity, it was assumed that the inputs and outputs are scalars. Then, for each layer, the set of parameters $\{a_l, b_l\}_{l=1}^L \cup \{c\}$ comprise the abc-parameterization to

- 1. Initialize and scale weight matrices at every layer as $\mathbf{W}_l = n^{-a_l}[\mathbf{w}_l^{(i,j)}]$, where $\mathbf{w}_l^{(i,j)} \sim \mathcal{N}(0, n^{-2b_l}\sigma^2)$
- 2. Scale the learning rate such that $\Delta \mathbf{W}_l = -\eta \ n^{-c} \ \Psi(\{\nabla_{\mathbf{W}_l} \mathcal{L}\})$

where the scale of initial variance, σ^2 , and the learning rate, η , is assumed to be width-independent. As emphasized in Section 1, the theoretical principles behind μP can be difficult to grasp. Recognizing these challenges, Yang et al. (2023a) provided the following equivalent conditions for μP

$$||\mathbf{h}_l(\mathbf{x})||_2 = \Theta(\sqrt{n_l})$$
 and $||\Delta \mathbf{h}_l||_2 = \Theta(\sqrt{n_l})$, for $l = 1, 2, \dots, L - 1$. (C.1.)

The above conditions concisely represent the requirements of μP .

3.2 Spectral Conditions for Feature Learning

In Yang et al. (2023a), the authors futher argued that conditions (C.1.) can be ensured by the following *spectral scaling conditions* on the weight matrices and their one step update,

$$||\mathbf{W}_l||_* = \Theta\left(\sqrt{\frac{n_l}{n_{l-1}}}\right)$$
 and $||\Delta \mathbf{W}_l||_* = \Theta\left(\sqrt{\frac{n_l}{n_{l-1}}}\right)$, for $l = 1, 2, \dots, L$. (C.2.)

The above spectral scaling conditions hold for any optimizer, and in the next section we present a framework to derive μ P for any arbitrary optimizer using conditions (C.2.).

4 Deriving μP using Spectral Scaling Conditions

As discussed in Section 3.1, deriving μP for a particular model and optimizer boils down to determining the scaling parameters in abc-parameterization, or an equivalent form. We propose a framework which only utilizes the spectral scaling conditions (C.2.) to derive the abc-parameterization. The typical approach to derive μP is to determine the proper scaling factors for a one step gradient update, and then argue recursively that for stable input vectors under μP , the output vectors are also stable, independent of the time.

4.1 GENERIC FRAMEWORK

Scaling of Model Weights and Initial Variance:

The scaling factors for the model weights and their initial variance, that is, akin to parameters $\{a_l,b_l\}_{l=1}^L$ in the abc-parameterization, can be computed by satisfying the condition on $||\mathbf{W}_l||_*$ in (C.2.). More rigorously, let us define the model weights as $\mathbf{W}_l = \sigma_l \tilde{\mathbf{W}}_l \in \mathbb{R}^{n_l \times n_{l-1}}$ where the elements of $\tilde{\mathbf{W}}_l$ are sampled from some initial distribution with scaled variance, $n^{-2b_l}\sigma^2$. For ease of theoretical analysis, we fix $b_l = 0$ for all layers. Then, $||\mathbf{W}_l||_* = \sigma_l ||\tilde{\mathbf{W}}_l||_*$. Since $||\tilde{\mathbf{W}}_l||_*$ is a random matrix with unit variance, existing results in random matrix theory can be leveraged to deduce the scaling of the spectral norm in terms of matrix dimensions (Rudelson & Vershynin (2010) Vershynin (2018)). Then, σ_l can be computed by equating $\sigma_l ||\tilde{\mathbf{W}}_l||_* = \Theta\left(\sqrt{n_l/n_{l-1}}\right)$.

Scaling of Learning Rate:

The scaling factor for the learning rate, akin to parameter c in abc-parameterization, is computed by satisfying the condition on $||\Delta \mathbf{W}_l||_*$ in (C.2.). This implies that the generic update rule in eq. (4) should be equated as,

$$||\Delta \mathbf{W}_l||_* = \eta(n_l)^{-c_1} (n_{l-1})^{-c_2} ||\Psi(\nabla_{\mathbf{W}_l} \mathcal{L})||_* = \Theta\left(\sqrt{\frac{n_l}{n_{l-1}}}\right),$$
 (5)

where the scaling constants c_1 and c_2 are determined based on the exact nature of $\Psi(\cdot)$.

	Input Weights	Output Weights	Hidden Weights
Init. Var.	$1\left(\frac{1}{n_{l-1}}\right)$	$1\left(\frac{1}{n_{l-1}^2}\right)$	$1\left(\frac{1}{n_{l-1}}\right)$
Multiplier	$\frac{1}{\sqrt{n_{l-1}}}$ (1)	$\frac{1}{n_{l-1}}$ (1)	$\frac{1}{\sqrt{n_{l-1}}}$ (1)
AdamW / ADOPT / Sophia LR	1 (1)	$\frac{1}{n_{l-1}} \left(\frac{1}{n_{l-1}} \right)$	$\frac{1}{n_{l-1}} \left(\frac{1}{n_{l-1}} \right)$
LAMB LR	1 (-)	1 (-)	1 (-)
Shampoo LR	$\sqrt{n_l}$ (-)	$\frac{1}{\sqrt{n_{l-1}}} \left(-\right)$	$\sqrt{\frac{n_l}{n_{l-1}}} \left(-\right)$

Table 2: Comparison of μ P from spectral conditions (black) vs. tensor programs ((Yang et al., 2021, Table 3)) (red).

Discussion: Observe that the scaling of model weights and initial variance is only dependent on the model architecture, not the optimization routine. Therefore, in the rest of this work we use the linear MLP described in Section 3 as our fixed model architecture and assume that the weights are initialized using standard normal distribution. Since the spectral norm of a random matrix with unit variance scales $\approx (\sqrt{n_l} + \sqrt{n_{l-1}})$, the appropriate scaling factor is computed to be σ_l

$$\Theta\left(\frac{1}{\sqrt{n_{l-1}}}\min\left\{1,\sqrt{\frac{n_l}{n_{l-1}}}\right\}\right)$$
 (Yang et al. (2023a)). Note that the initial variance is fixed as 1 for

the ease of theoretical analysis. In practice, to increase numerical stability, the variance can be set to σ_L^2 while the weight multiplier can be fixed to 1 for normal distribution.

Further, observe that eq. (5) computes separate scaling factors for the input and output dimensions of the weight matrices, that is, using spectral scaling conditions to derive μP allows us to collectively analyze the different types of layers (input, output and hidden layers). We recommend first determining the scaling factors c_1 and c_2 by removing additional HPs, such as weight-decay, epsilon for numerical stability etc., from the update rule because they typically do not have a comparable order

of magnitude to other terms. In case of low-precision training (Blake et al. (2025a)), these HPs can be scaled after c_1 and c_2 have been computed, as demonstrated at the end of Section 4.2.

Finally, we want to highlight that while there is no difference in the correctness and rigor of using either a tensor programming approach or the proposed spectral scaling approach, the latter is more intuitive and therefore, makes it easier to adopt and reason about μP for a wide class of optimizers. Additionally, the rich literature on spectral norms and their properties which can be leveraged to analyze different adaptive optimization routines, as will be demonstrated in the following sections.

In Section 4.2, we first demonstrate how to utilize the above framework by deriving μP for AdamW, and corroborate our results with the μP scalings reported in literature (Yang et al. (2021)). We then derive μP for optimizers - ADOPT, LAMB, Sophia and Shampoo, which have shown promising results for training LLMs. Our results are summarized in Table 2 and in Result 4.1. Figs. 2 and 3 demonstrate zero-shot learning rate transfer across model widths for different optimizers, under the derived μP scalings. Note that we do not need additional assumptions for deriving μP for the model described in Section 3. However, to extend μP to more realistic models, we make the same assumptions as in (Yang et al. (2023a)), which are listed in Appendix A.

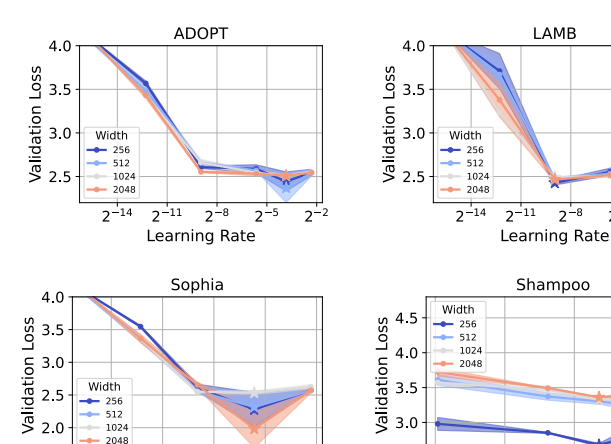


Figure 2: (NanoGPT) Mean validation loss for increasing model width and different learning rates across four optimizers: ADOPT (top left), LAMB (top right), Sophia (bottom left), and Shampoo (bottom right). The plots demonstrate zero-shot learning rate transfer under μ P (Table 2)

Besult: Under standing assumptions, for a linear MLP with L

Result: Under standing assumptions, for a linear MLP with L layers, if the weight matrices $\mathbf{W}_l = \sigma_l \tilde{\mathbf{W}}_l$, l = 1, 2, ... L are initialized as $\tilde{\mathbf{W}}_{i,j} \sim \mathcal{N}(0, 1)$, then the spectral conditions (C.2.) are satisfied for AdamW, ADOPT and Sophia if

$$\sigma_l = \Theta\left(\frac{1}{\sqrt{n_{l-1}}} \min\left\{1, \sqrt{\frac{n_l}{n_{l-1}}}\right\}\right); \qquad \quad \eta = \Theta\left(\frac{1}{n_{l-1}}\right),$$

$$\begin{aligned} \text{for LAMB if} \\ \sigma_{l} &= \Theta\left(\frac{1}{\sqrt{n_{l-1}}} \min\left\{1, \sqrt{\frac{n_{l}}{n_{l-1}}}\right\}\right); \end{aligned} \qquad \eta = \Theta\left(1\right),$$

and for Shampoo if

$$\sigma_l = \Theta\left(\frac{1}{\sqrt{n_{l-1}}}\min\left\{1, \sqrt{\frac{n_l}{n_{l-1}}}\right\}\right); \qquad \quad \eta = \Theta\left(\sqrt{\frac{n_l}{n_{l-1}}}\right),$$

where $n_{l-1} = 1$ for input weights and $n_l = 1$ for output weights.

Remark 1 For a linear MLP trained with a batch size of 1, the gradient matrix is a rank one matrix because it can be written as an outer product of two vectors, $\nabla_{\mathbf{W}_{l}}\mathcal{L} = \nabla_{\mathbf{h}_{l}}\mathcal{L} \cdot \mathbf{h}_{l-1}^{T}$. Therefore, $||\nabla_{\mathbf{W}_{l}}\mathcal{L}||_{*} = ||\nabla_{\mathbf{W}_{l}}\mathcal{L}||_{F}$ from property (1). (See discussion in (Yang et al., 2023a, p. 9))

Remark 2 For a linear MLP trained with a batch size of 1, it can be shown using first order Taylor series expansion that $||\nabla_{\mathbf{W}_{l}}\mathcal{L}||_{*} = \Theta(\sqrt{\frac{n_{l-1}}{n_{l}}})$ (Yang et al., 2023a, p. 9). Further, since $\nabla_{\mathbf{W}_{l}}\mathcal{L}$ is

a rank one matrix, $||\nabla_{\mathbf{W}_l}\mathcal{L}||_* = ||\nabla_{\mathbf{h}_l}\mathcal{L}||_2 ||\mathbf{h}_{l-1}||_2 = ||\nabla_{\mathbf{h}_l}\mathcal{L}||_2 \Theta(\sqrt{n_{l-1}})$, using property (1) and condition (C.1.). Then, $||\nabla_{\mathbf{h}_l}\mathcal{L}||_2 = \Theta(1/\sqrt{n_l})$.

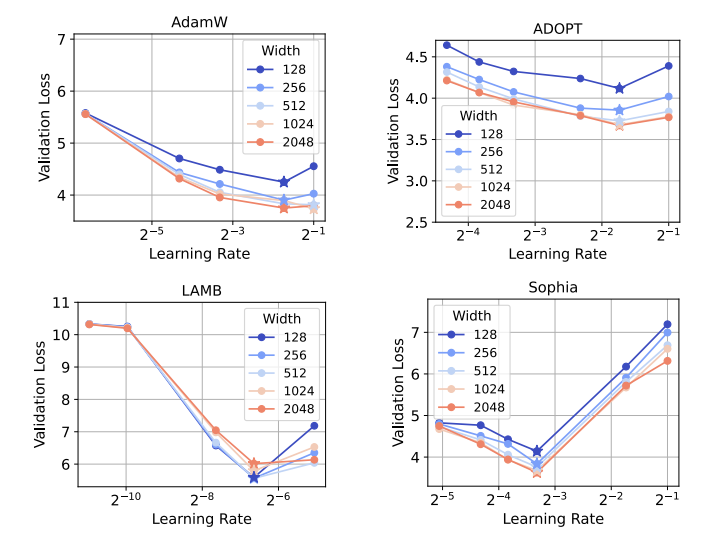


Figure 3: (Llama2) Validation loss for increasing model width and different learning rates across four optimizers: AdamW (top left), ADOPT (top right), LAMB (bottom left), and Sophia (bottom right). The plots demonstrate zero-shot learning rate transfer under μ P (Table 2).

4.2 μ P FOR ADAMW

Recall the update rule for AdamW (Loshchilov & Hutter (2017)),

$$\mathbf{W}_{l}^{(t+1)} = \mathbf{W}_{l}^{(t)} - \eta^{(t)} \left(\frac{\hat{\mathbf{m}}^{(t)}}{\sqrt{\hat{\mathbf{v}}^{(t)}} + \epsilon} + \lambda \mathbf{W}_{l}^{(t)} \right) \tag{AdamW}$$
where
$$\hat{\mathbf{m}}^{(t)} = \frac{\mathbf{m}^{(t)}}{(1 - \beta_{1}^{t})} = \frac{1}{(1 - \beta_{1}^{t})} \left[\beta_{1} \mathbf{m}^{(t-1)} + (1 - \beta_{1}) \nabla_{\mathbf{W}_{l}^{(t)}} \mathcal{L} \right] ; \quad \mathbf{m}^{(0)} = 0$$

$$\hat{\mathbf{v}}^{(t)} = \frac{\mathbf{v}^{(t)}}{(1 - \beta_{2}^{t})} = \frac{1}{(1 - \beta_{2}^{t})} \left[\beta_{2} \mathbf{v}^{(t-1)} + (1 - \beta_{2}) (\nabla_{\mathbf{W}_{l}^{(t)}} \mathcal{L})^{2} \right] ; \quad \mathbf{v}^{(0)} = 0$$

From the spectral scaling condition in eq. (5), we need to find $c_1, c_2 \in \mathbb{R}$ such that

$$||\Delta \mathbf{W}_l||_* = \eta(n_l)^{-c_1} (n_{l-1})^{-c_2} \left\| \frac{\hat{\mathbf{m}}}{\sqrt{\hat{\mathbf{v}}} + \epsilon} + \lambda \mathbf{W}_l \right\|_* = \Theta\left(\sqrt{\frac{n_l}{n_{l-1}}}\right). \tag{6}$$

Similar to previous works, we first analyze AdamW for $\beta_1 = \beta_2 = \epsilon = 0$. Then, the above update rule reduces to signSGD (Bernstein et al. (2018)). Additionally, since the gradient term dominates the weight decay term, we ignore the latter because we are only concerned with an order-of-magnitude calculation. Therefore, (6) reduces to

$$||\Delta \mathbf{W}_l||_* = \eta(n_l)^{-c_1}(n_{l-1})^{-c_2}||\mathrm{sign}(\nabla_{\mathbf{W}_l}\mathcal{L})||_* \approx \eta(n_l)^{-c_1}(n_{l-1})^{-c_2}||\mathrm{sign}(\nabla_{\mathbf{W}_l}\mathcal{L})||_{\mathrm{F}}$$

where the last equation follows from Remark 1. From the definition of the Frobenius norm, we have $||\mathbf{1}_{n_l \times n_{l-1}}||_F^2 = \sum_{i=1}^{n_l} \sum_{j=i}^{n_{l-1}} 1 = n_l n_{l-1}$. This gives

$$||\Delta \mathbf{W}_l||_* = \eta(n_l)^{-c_1} (n_{l-1})^{-c_2} \Theta\left(\sqrt{n_l n_{l-1}}\right) = \Theta\left(n_l^{1/2-c_1} n_{l-1}^{1/2-c_2}\right).$$

By fixing $c_1=0$ and $c_2=1$, the spectral scaling condition in eq.(5) is satisfied. Therefore, the learning rate for AdamW should be scaled by a factor of $1/n_{l-1}$. Observe that this scaling is consistent with the μP derived using the tensor programming approach (Yang et al., 2021, Table 3), and this equivalence is highlighted in Table 2. Fig. 4 further validates our derivation via the coordinate check plots and the "wider is better" phenomenon observed in the plot on the right.

Scaling the Weight Decay Parameter:

Observe that for the derived μP scaling to hold for (AdamW), the spectral norm of the weight decay term, $||\lambda \mathbf{W}_l||_*$, must have the same order of magnitude as the spectral norm of the gradient term, which is $\Theta(\sqrt{n_l n_{l-1}})$. Since, $||\lambda \mathbf{W}_l||_* = \lambda ||\mathbf{W}_l||_* = \lambda \Theta(\sqrt{n_l / n_{l-1}})$, where the last equality follows from condition (C.2.), then λ should be scaled by a factor of n_{l-1} . This result is consistent with Table 1 in Dey et al. (2025).

4.3 μP FOR ADOPT

Recall that the update rule for ADOPT is the same as AdamW. The key difference lies in the sequence in which the terms $\hat{\mathbf{m}}^{(t)}$ and $\hat{\mathbf{v}}^{(t)}$ are updated (Taniguchi et al. (2024)). From a theoretical perspective, this does not change the order of magnitude of the gradient function $\Psi(\{\nabla_{\mathbf{W}_l}\mathcal{L}\})$ from that of AdamW, and hence, the parameterization derived for AdamW also holds for ADOPT.

4.4 μ P FOR LAMB

Recall the update rule for LAMB (You et al. (2019)),

$$\mathbf{W}_{l}^{(t+1)} = \mathbf{W}_{l}^{(t)} - \eta^{(t)} \frac{\phi(||\mathbf{W}_{l}^{(t)}||_{F})}{||\mathbf{r}_{l}^{(t)} + \lambda \mathbf{W}_{l}^{(t)}||_{F}} \left(\mathbf{r}_{l}^{(t)} + \lambda \mathbf{W}_{l}^{(t)}\right)$$
(LAMB)

where $\mathbf{r}_l^{(t)} = \frac{\hat{\mathbf{m}}^{(t)}}{\sqrt{\hat{\mathbf{v}}^{(t)} + \epsilon}}$. In (LAMB), the gradient in each layer of the model is scaled by terms of orders $\frac{||\mathbf{W}_l||_F}{||\mathbf{r} + \lambda \mathbf{W}||_F}$. From condition (C.1.), we know

$$||\mathbf{W}_l||_F pprox ||\mathbf{W}_l||_* = \Theta\left(\sqrt{rac{n_l}{n_{l-1}}}
ight) \qquad ext{and} \qquad ||\mathbf{r}_l + \lambda \mathbf{W}_l||_{\mathrm{F}} = \Theta\left(\sqrt{n_l n_{l-1}}
ight)$$

if we ignore the weight decay term and set $\beta_1=\beta_2=\epsilon=0$. Then, from the spectral scaling condition in eq. (5), we need to find $c_1,c_2\in\mathbb{R}$ such that

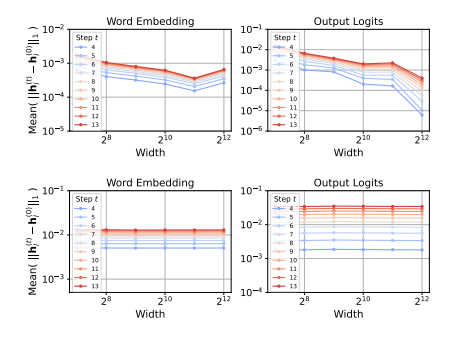
$$||\Delta \mathbf{W}||_{*} \approx \eta(n_{l})^{-c_{1}} (n_{l-1})^{-c_{2}} \Theta\left(\frac{1}{n_{l-1}}\right) ||\mathbf{r}_{l} + \lambda \mathbf{W}_{l}||_{F}$$

$$= \eta(n_{l})^{-c_{1}} (n_{l-1})^{-c_{2}} \Theta\left(\frac{1}{n_{l-1}}\right) \Theta\left(\sqrt{n_{l} n_{l-1}}\right)$$

$$= \eta(n_{l})^{-c_{1}} (n_{l-1})^{-c_{2}} \Theta\left(\sqrt{\frac{n_{l}}{n_{l-1}}}\right)$$

where the second equality follows using the same reasoning as for AdamW. Then condition (5) holds if $c_1 = c_2 = 0$.

Insight 1 The above derivation suggests that the update rule for LAMB is implicitly independent of width scaling. Intuitively, this result holds because the layerwise gradient scaling in (LAMB) causes the effective learning rate to be different for each layer.



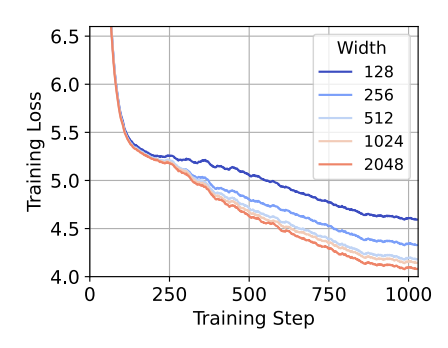


Figure 4: (Llama2 model) AdamW optimizer - Coordinate check plots under standard parameterization (top left) and under μ P (bottom left) for the word embedding and output logits layers; Decreasing training loss with increasing model width under μ P (right).

4.5 SOPHIA

Recall the update rule for Sophia (Liu et al. (2023)),

$$\mathbf{W}_{l}^{(t+1)} = \mathbf{W}_{l}^{(t)} - \eta^{(t)} \operatorname{clip}\left(\frac{\mathbf{m}^{(t)}}{\max\{\gamma \mathbf{h}^{(t)}, \epsilon\}}, 1\right) - \eta^{(t)} \lambda \mathbf{W}_{l}^{(t)}$$
 (Sophia)

where $\mathbf{h}^{(t)}$ is a momentum-based estimate of the diagonal vector of the Hessian at time t. From the spectral scaling condition in (5), we need to find $c_1, c_2 \in \mathbb{R}$ such that

$$||\Delta \mathbf{W}_l||_* = \eta(n_l)^{-c_1} (n_{l-1})^{-c_2} \left\| \operatorname{clip} \left(\frac{\mathbf{m}^{(t)}}{\max \left\{ \gamma \mathbf{h}^{(t)}, \epsilon \right\}}, 1 \right) - \lambda \mathbf{W}_l^{(t)} \right\|_* = \Theta \left(\sqrt{\frac{n_l}{n_{l-1}}} \right).$$

For analysis, we consider $\beta_1 = \beta_2 = \epsilon = 0$, and since the weight decay term is usually very small, the above weight update simplifies to

$$\begin{aligned} ||\Delta \mathbf{W}_l||_* &= \eta(n_l)^{-c_1} (n_{l-1})^{-c_2} \left\| \operatorname{clip} \left(\frac{\nabla_{\mathbf{W}_l} \mathcal{L}}{\gamma \nabla_{\mathbf{W}_l}^2 \mathcal{L}}, 1 \right) \right\|_* \\ &= \eta(n_l)^{-c_1} (n_{l-1})^{-c_2} \left\| \operatorname{clip} \left(\frac{1}{\gamma |\nabla_{\mathbf{W}_l} \mathcal{L}|}, 1 \right) \right\|_* \\ &\approx \eta(n_l)^{-c_1} (n_{l-1})^{-c_2} \left\| \operatorname{clip} \left(\frac{1}{\gamma |\nabla_{\mathbf{W}_l} \mathcal{L}|}, 1 \right) \right\|_{\mathrm{F}} \end{aligned}$$

where in the second equality we take the modulus of the gradient term in the denominator because Sophia avoids negative diagonal terms in the Hessian (thereby avoiding convergence to a saddle point; see discussion in (Liu et al., 2023, pg. 6)). Observe that the clip $(\cdot,1)$ bounds the coordinate-wise weight updates as, $|[\Delta \mathbf{W}_l]_{i,j}| \leq 1$. Therefore, we can compute an upper bound for the Frobenius norm and get

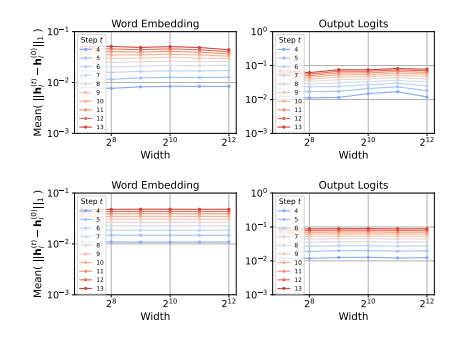
$$||\Delta \mathbf{W}_l||_* \le \eta(n_l)^{-c_1} (n_{l-1})^{-c_2} \frac{1}{\gamma} \Theta(\sqrt{n_l n_{l-1}}).$$

Then, eq. (5) is satisfied by fixing $c_1 = 0$ and $c_2 = 1$, resulting in the same μP scaling as AdamW.

Insight 2 Intuitively, it is easy to see why this result holds. Sophia uses signSGD as the default method to handle negative Hessian terms (to avoid convergence to a saddle point), thereby mirroring the analysis for AdamW for such cases. Additionally, when $\gamma=1$, all the elements in the weight update are clipped to 1, and the upper bound holds exactly. Thus, we get the same scaling as AdamW.

In practice, the authors suggest to choose γ such that 10% - 50% of the parameters are not clipped. Therefore, for each term which is not clipped, the above bound incurs an error of less than 1. However, as demonstrated in our simulations (Fig. 2), for the typical values of γ used in practice, the μP scaling derived based on the above calculation works well.

Fig. 5 further validates the μ P derivation for Sophia via stable coordinate check plots (Fig. 5 (left)) and a consistently improving training loss across model widths (Fig. 5(right)).



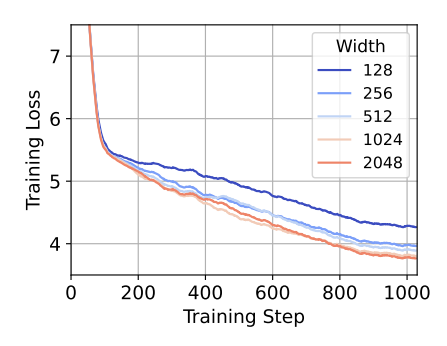


Figure 5: (Llama2 model) Sophia optimizer - Coordinate check plots under standard parameterization (top left) and under μ P (bottom left) for the word embedding and output logits layers; Decreasing training loss with increasing model width under μ P (right).

4.6 μ P for Shampoo

Recall the update rule for Shampoo (Gupta et al. (2018)),

$$\mathbf{W}_{l}^{(t+1)} = \mathbf{W}_{l}^{(t)} - \eta \left(\mathbf{L}_{l}^{(t)}\right)^{-1/4} \nabla_{\mathbf{W}_{l}} \mathcal{L}\left(\mathbf{R}_{l}^{(t)}\right)^{-1/4} \tag{Shampoo}$$

where for some
$$\delta > 0$$
, $\mathbf{L}_l^{(t)} = \mathbf{L}_l^{(t-1)} + \nabla_{\mathbf{W}_l} \mathcal{L} \cdot \nabla_{\mathbf{W}_l} \mathcal{L}^{\mathrm{T}}$; $\mathbf{L}_l^{(0)} = \delta \mathbf{I} \in \mathbb{R}^{n_l \times n_l}$
 $\mathbf{R}_l^{(t)} = \mathbf{R}_l^{(t-1)} + \nabla_{\mathbf{W}_l} \mathcal{L}^{\mathrm{T}} \cdot \nabla_{\mathbf{W}_l} \mathcal{L}$; $\mathbf{R}_l^{(0)} = \delta \mathbf{I} \in \mathbb{R}^{n_{l-1} \times n_{l-1}}$

From the spectral scaling condition in (5), we need to find $c_1, c_2 \in \mathbb{R}$ such that

$$||\Delta \mathbf{W}_l||_* = \eta(n_l)^{-c_1} (n_{l-1})^{-c_2} \left\| \left(\mathbf{L}_l^{(t)} \right)^{-1/4} \nabla_{\mathbf{W}_l} \mathcal{L} \left(\mathbf{R}_l^{(t)} \right)^{-1/4} \right\|_* = \Theta \left(\sqrt{\frac{n_l}{n_{l-1}}} \right).$$

For one-step analysis, let $\delta = 0$. Then the above condition reduces to

$$\begin{split} ||\Delta \mathbf{W}_{l}||_{*} &= \eta(n_{l})^{-c_{1}}(n_{l-1})^{-c_{2}} \left\| \left(\nabla_{\mathbf{W}_{l}} \mathcal{L} \cdot \nabla_{\mathbf{W}_{l}} \mathcal{L}^{\mathsf{T}} \right)^{-1/4} \nabla_{\mathbf{W}_{l}} \mathcal{L} \left(\nabla_{\mathbf{W}_{l}} \mathcal{L}^{\mathsf{T}} \cdot \nabla_{\mathbf{W}_{l}} \mathcal{L} \right)^{-1/4} \right\|_{*} \\ &\leq \eta(n_{l})^{-c_{1}}(n_{l-1})^{-c_{2}} \left\| \left(\nabla_{\mathbf{W}_{l}} \mathcal{L} \cdot \nabla_{\mathbf{W}_{l}} \mathcal{L}^{\mathsf{T}} \right)^{-1/4} \right\|_{*} \left\| \nabla_{\mathbf{W}_{l}} \mathcal{L}\|_{*} \left\| \left(\nabla_{\mathbf{W}_{l}} \mathcal{L}^{\mathsf{T}} \cdot \nabla_{\mathbf{W}_{l}} \mathcal{L} \right)^{-1/4} \right\|_{*} \\ &= 2 \eta \left((n_{l})^{-c_{1}}(n_{l-1})^{-c_{2}} \Theta \left(\sqrt{\frac{n_{l-1}}{n_{l}}} \right) \left\| \left(\nabla_{\mathbf{W}_{l}} \mathcal{L} \cdot \nabla_{\mathbf{W}_{l}} \mathcal{L}^{\mathsf{T}} \right)^{-1/4} \right\|_{*} \left\| \left((\mathbf{h}_{l-1} \cdot \nabla_{\mathbf{h}_{l}} \mathcal{L}^{\mathsf{T}} \nabla_{\mathbf{h}_{l}} \mathcal{L} \cdot \mathbf{h}_{l-1}^{\mathsf{T}} \right)^{-1/4} \right\|_{*} \\ &= \eta \Theta \left((n_{l})^{-c_{1}-\frac{1}{2}}(n_{l-1})^{-c_{2}+\frac{1}{2}} \right) \left\| \left((\mathbf{h}_{l-1})^{-l} \mathcal{L}^{\mathsf{T}} \nabla_{\mathbf{h}_{l}} \mathcal{L}^{\mathsf{T}} \right)^{-1/4} \right\|_{*} \left\| \left((\mathbf{h}_{l-1} \cdot \nabla_{\mathbf{h}_{l}} \mathcal{L}^{\mathsf{T}} \nabla_{\mathbf{h}_{l}} \mathcal{L} \cdot \mathbf{h}_{l-1}^{\mathsf{T}} \right)^{-1/4} \right\|_{*} \\ &= \eta \Theta \left((n_{l})^{-c_{1}-\frac{1}{2}}(n_{l-1})^{-c_{2}+\frac{1}{2}} \right) \left\| \left((\mathbf{h}_{l-1})^{-l} \mathcal{L}^{\mathsf{T}} \nabla_{\mathbf{h}_{l}} \mathcal{L}^{\mathsf{T}} \right)^{-1/4} \right\|_{*} \left\| \left((\mathbf{h}_{l-1} \cdot \mathbf{h}_{l-1}^{\mathsf{T}} \right)^{-1/4} \right\|_{*} \\ &= \eta \Theta \left((n_{l})^{-c_{1}-\frac{1}{2}}(n_{l-1})^{-c_{2}+\frac{1}{2}} \right) \Theta(n_{l-1}^{-1/4}) \left\| \left((\nabla_{\mathbf{h}_{l}} \mathcal{L} \cdot \nabla_{\mathbf{h}_{l}} \mathcal{L}^{\mathsf{T}} \right)^{-1/4} \right\|_{*} \left\| \left((\mathbf{h}_{l-1} \cdot \mathbf{h}_{l-1}^{\mathsf{T}} \right)^{-1/4} \right\|_{*} \\ &= \eta \Theta \left((n_{l})^{-c_{1}-\frac{1}{2}}(n_{l-1})^{-c_{2}+\frac{1}{2}} \right) \Theta(n_{l-1}^{-1/4}) \left\| \left((\nabla_{\mathbf{h}_{l}} \mathcal{L} \cdot \nabla_{\mathbf{h}_{l}} \mathcal{L}^{\mathsf{T}} \right)^{-1/4} \right\|_{*} \left\| \left((\mathbf{h}_{l-1} \cdot \mathbf{h}_{l-1}^{\mathsf{T}} \right)^{-1/4} \right\|_{*} \\ &= \eta \Theta \left((n_{l})^{-c_{1}-\frac{1}{4}}(n_{l-1})^{-c_{2}+\frac{1}{4}} \right) \left\| \left((\nabla_{\mathbf{h}_{l}} \mathcal{L} \cdot \nabla_{\mathbf{h}_{l}} \mathcal{L}^{\mathsf{T}} \right)^{-1/4} \right\|_{*} \left\| \left((\mathbf{h}_{l-1} \cdot \mathbf{h}_{l-1}^{\mathsf{T}} \right)^{-1/4} \right\|_{*} \\ &= \eta \Theta \left((n_{l})^{-c_{1}-\frac{1}{4}}(n_{l-1})^{-c_{2}+\frac{1}{4}} \right) \left\| \left((\nabla_{\mathbf{h}_{l}} \mathcal{L} \cdot \nabla_{\mathbf{h}_{l}} \mathcal{L}^{\mathsf{T}} \right)^{-1/4} \right\|_{*} \left\| \left((\mathbf{h}_{l-1} \cdot \mathbf{h}_{l-1}^{\mathsf{T}} \right)^{-1/4} \right\|_{*} \\ &= \eta \Theta \left((n_{l})^{-c_{1}-\frac{1}{4}}(n_{l-1})^{-c_{2}+\frac{1}{4}} \right) \Theta(n_{l}^{-1/4}) \Theta(n_{l-1}^{-1/4}) \\ &= \eta \Theta \left((n_{l})^{-c_{1}-\frac{1}{4}}(n_{l-1})^{-c_{2}+$$

where (1) follows from sub-multiplicative property of matrix norms, (2) follows from Remark 2, (3) and (5) follow from condition (C.1.) and Remark 2, (4) follows from property (1) and property (2). Therefore, condition (5) is satisfied by fixing $c_1 = -1/2$ and $c_2 = 1/2$.

5 Numerical Results

We test and validate our derivations on the NanoGPT model (Karpathy (2022)) and the Llama2 model (Touvron et al. (2023)). As demonstrated in Figs. 2 and 3, our simulation results validate the μ P derivations in Table 2 across the different optimizers. Extensive numerical results, including training settings, HP values, depth scaling studies, and validation loss values for the different optimizers and model sizes can be found in Appendix B. The simulations on NanoGPT were performed using four A100 GPUs of the Argonne Leadership Computing Facility's Polaris supercomputer (Leadership Computing Facility (b)), while the simulations on Llama2 were performed using 12 Intel Data Center GPU Max Series on the Aurora supercomputer (Leadership Computing Facility (a)).

6 Conclusion

We have proposed a novel framework to derive μP using spectral scaling conditions, which are more intuitive and easier to work with than the prevalent tensor programs. Using the proposed framework, we have derived μP for a wide range of adaptive, first and second-order optimizers including, AdamW, ADOPT, LAMB, Sophia, and Shampoo. We have validated our derivations in simulation and by demonstrating zero-shot learning rate transfer on NanoGPT and Llama2 models. Motivated by our depth-scaling simulations (Appendix B), we aim to develop a sound theoretical framework for depth-scaling parameterization in the future.

REFERENCES

Jeremy Bernstein, Yu-Xiang Wang, Kamyar Azizzadenesheli, and Animashree Anandkumar. signsgd: Compressed optimisation for non-convex problems. In *International conference on ma-*

- chine learning, pp. 560-569. PMLR, 2018. URL https://doi.org/10.48550/arXiv. 1802.04434.
 - Charlie Blake, Constantin Eichenberg, Josef Dean, Lukas Balles, Luke Yuri Prince, Björn Deiseroth, Andres Felipe Cruz-Salinas, Carlo Luschi, Samuel Weinbach, and Douglas Orr. u-\$\mu\$p: The unit-scaled maximal update parametrization. In *The Thirteenth International Conference on Learning Representations*, 2025a. URL https://openreview.net/forum?id=P7KRIiLM8T.
 - Charlie Blake, Constantin Eichenberg, Josef Dean, Lukas Balles, Luke Yuri Prince, Björn Deiseroth, Andres Felipe Cruz-Salinas, Carlo Luschi, Samuel Weinbach, and Douglas Orr. u- μ p: The unit-scaled maximal update parametrization. In *The Thirteenth International Conference on Learning Representations*, 2025b.
 - Nolan Dey, Bin Claire Zhang, Lorenzo Noci, Mufan Li, Blake Bordelon, Shane Bergsma, Cengiz Pehlevan, Boris Hanin, and Joel Hestness. Don't be lazy: Completep enables compute-efficient deep transformers. *arXiv preprint arXiv:2505.01618*, 2025. URL https://doi.org/10.48550/arXiv.2505.01618.
 - Vineet Gupta, Tomer Koren, and Yoram Singer. Shampoo: Preconditioned stochastic tensor optimization. In *International Conference on Machine Learning*, pp. 1842–1850. PMLR, 2018. URL https://doi.org/10.48550/arXiv.1802.09568.
 - Satoki Ishikawa and Ryo Karakida. On the parameterization of second-order optimization effective towards the infinite width. In *The Twelfth International Conference on Learning Representations*.
 - Keller Jordan, Yuchen Jin, Vlado Boza, Jiacheng You, Franz Cesista, Laker Newhouse, and Jeremy Bernstein. Muon: An optimizer for hidden layers in neural networks. *Cited on*, pp. 10, 2024. URL https://kellerjordan.github.io/posts/muon/.
 - Andrej Karpathy. NanoGPT. https://github.com/karpathy/nanoGPT, 2022.
 - Argonne Leadership Computing Facility. Aurora. https://www.alcf.anl.gov/aurora,a.
 - Argonne Leadership Computing Facility. Polaris. https://www.alcf.anl.gov/polaris, b.
 - Hong Liu, Zhiyuan Li, David Hall, Percy Liang, and Tengyu Ma. Sophia: A scalable stochastic second-order optimizer for language model pre-training. *arXiv* preprint arXiv:2305.14342, 2023. URL https://doi.org/10.48550/arXiv.2305.14342.
 - Jingyuan Liu, Jianlin Su, Xingcheng Yao, Zhejun Jiang, Guokun Lai, Yulun Du, Yidao Qin, Weixin Xu, Enzhe Lu, Junjie Yan, et al. Muon is scalable for llm training. *arXiv preprint arXiv:2502.16982*, 2025. URL https://doi.org/10.48550/arXiv.2502.16982.
 - Ilya Loshchilov and Frank Hutter. Decoupled weight decay regularization. *arXiv preprint arXiv:1711.05101*, 2017. URL https://doi.org/10.48550/arXiv.1711.05101.
 - Carl D Meyer. Matrix analysis and applied linear algebra. SIAM, 2023.
 - Mark Rudelson and Roman Vershynin. Non-asymptotic theory of random matrices: extreme singular values. In *Proceedings of the International Congress of Mathematicians 2010 (ICM 2010) (In 4 Volumes) Vol. I: Plenary Lectures and Ceremonies Vols. II–IV: Invited Lectures*, pp. 1576–1602. World Scientific, 2010.
 - Gilbert Strang. Linear algebra and its applications. 2012.
 - Shohei Taniguchi, Keno Harada, Gouki Minegishi, Yuta Oshima, Seong Cheol Jeong, Go Nagahara, Tomoshi Iiyama, Masahiro Suzuki, Yusuke Iwasawa, and Yutaka Matsuo. Adopt: Modified adam can converge with any β_2 with the optimal rate. Advances in Neural Information Processing Systems, 37:72438–72474, 2024. URL https://doi.org/10.48550/arXiv.2411.02853.

Benjamin Thérien, Charles-Étienne Joseph, Boris Knyazev, Edouard Oyallon, Irina Rish, and Eugene Belilovsky. μ lo: Compute-efficient meta-generalization of learned optimizers. In *OPT* 2024: Optimization for Machine Learning. URL https://doi.org/10.48550/arXiv. 2406.00153.

Hugo Touvron, Louis Martin, Kevin Stone, Peter Albert, Amjad Almahairi, Yasmine Babaei, Nikolay Bashlykov, Soumya Batra, Prajjwal Bhargava, Shruti Bhosale, et al. Llama 2: Open foundation and fine-tuned chat models. *arXiv preprint arXiv:2307.09288*, 2023.

- Roman Vershynin. *High-dimensional probability: An introduction with applications in data science*, volume 47. Cambridge university press, 2018.
- Greg Yang and Edward J Hu. Feature learning in infinite-width neural networks. *arXiv preprint arXiv:2011.14522*, 2020. URL https://doi.org/10.48550/arXiv.2011.14522.
- Greg Yang, Edward Hu, Igor Babuschkin, Szymon Sidor, Xiaodong Liu, David Farhi, Nick Ryder, Jakub Pachocki, Weizhu Chen, and Jianfeng Gao. Tuning large neural networks via zero-shot hyperparameter transfer. *Advances in Neural Information Processing Systems*, 34:17084–17097, 2021. URL https://doi.org/10.48550/arXiv.2203.03466.
- Greg Yang, James B Simon, and Jeremy Bernstein. A spectral condition for feature learning. *arXiv* preprint arXiv:2310.17813, 2023a. URL https://doi.org/10.48550/arXiv.2310.17813.
- Greg Yang, Dingli Yu, Chen Zhu, and Soufiane Hayou. Tensor programs vi: Feature learning in infinite-depth neural networks. *arXiv preprint arXiv:2310.02244*, 2023b. URL https://doi.org/10.48550/arXiv.2310.02244.
- Yang You, Jing Li, Sashank Reddi, Jonathan Hseu, Sanjiv Kumar, Srinadh Bhojanapalli, Xiaodan Song, James Demmel, Kurt Keutzer, and Cho-Jui Hsieh. Large batch optimization for deep learning: Training bert in 76 minutes. *arXiv preprint arXiv:1904.00962*, 2019. URL https://doi.org/10.48550/arXiv.1904.00962.
- Chenyu Zheng, Xinyu Zhang, Rongzhen Wang, Wei Huang, Zhi Tian, Weilin Huang, Jun Zhu, and Chongxuan Li. Scaling diffusion transformers efficiently via \$\sqrt{mup.} arXiv preprint arXiv:2505.15270, 2025.

A ASSUMPTIONS

To extend the derivations in Section 4 to more practical models, we use the following assumptions.

Assumption 1 *The weight updates do not cancel initial quantities.*

$$||\mathbf{W}_l + \Delta \mathbf{W}_l||_* = \Theta(||\mathbf{W}_l||_* + ||\Delta \mathbf{W}_l||_*)$$

$$||\mathbf{h}_l(\mathbf{x}) + \Delta \mathbf{h}_l(\mathbf{x})||_* = \Theta(||\mathbf{h}_l(\mathbf{x})||_* + ||\Delta \mathbf{h}_l(\mathbf{x})||_*).$$

Assumption 1 is used to deal with additional gradient steps.

Assumption 2 If a nonlinear activation function $\phi(\cdot)$ is added to each layer of the MLP, then

$$||\phi(\mathbf{h}_l(\mathbf{x}))||_2 = \Theta(||\mathbf{h}_l(\mathbf{x})||_2).$$

In other words, assumption 2 ensures that the order of magnitude of the inputs and outputs of an activation function are the same.

So far in our derivations, we assume that the batch size is 1. In practice, if a batch size of $B \in \mathbb{R}$ is used then for our calculations to hold, we need the following two assumptions. Observe that assumption 3 plays the same role as assumption 1.

Assumption 3

$$\|\Delta \mathbf{W}_l \mathbf{h}_l(\mathbf{x}_i)\|_2 = \Theta\left(\left\|\frac{1}{B}\Delta \mathbf{W}_l^{(i)} \mathbf{h}_l(\mathbf{x}_i)\right\|_2\right).$$

Assumption 4 The batch size is independent of the width, that is $B = \Theta(1)$.

B SIMULATIONS

Consistent with existing literature, we first verify μP for ADOPT, Sophia, LAMB and Shampoo optimizers by implementing the derived parameterization scheme (Table 2) in the NanoGPT codebase Karpathy (2022). Although prior works have already implemented μP for AdamW, we present the results again for completeness. Table 3 lists some of the settings for our experimental setup to test μP on NanoGPT. Further, we demonstrate the effectiveness for AdamW, ADOPT, LAMB and Sophia on the Llama2 model, the experimental setup for which is listed in Table 15.

We also present simulation results for depth-scaling parameterization for the above optimizers on NanoGPT, using the implementation suggested in Yang et al. (2023b) and dey2025don. Note that deriving proper depth-scaling parameterization for different optimizers is an ongoing work, and we only present preliminary results on the NanoGPT codebase in Section B.2 to motivate further theoretical analysis. Table 4 lists some of the settings for our experimental setup to test the depth-scaling parameterization.

The remainder of this section documents the simulation results for AdamW (Subsection B.2.1 and Subsection B.3.1), ADOPT (Subsection B.2.2 and Subsection B.3.2), Sophia (Subsection B.2.3 and Subsection B.3.4), LAMB (Subsection B.2.4 and Subsection B.3.3) and Shampoo (Subsection B.2.5) optimizers. For each optimizer we first present the coordinate check plots under standard parameterization, μ P and depth-scaling parameterization. These plots serve as a quick implementation check to monitor whether the weights blow-up, diminish to zero or remain stable with increasing model size (see discussion in (Yang et al., 2021, Section D.1, pg. 27)). We then provide tables and plots listing the validation loss for different learning rates, and increasing model width and model depth. The values in the tables for NanoGPT are the average loss values observed over multiple runs. While we do not document the standard deviations in the tables, they are highlighted in the plots. Note that since we are using an early stopping criterion for simulations performed on NanoGPT, we rely more on the observations gained from the validation loss data than the training loss data. Similar validation loss tables are documented for simulations performed on Llama2.

B.1 DISCUSSIONS

Overall, it is observed that the implementation of μP following Table 2 is quite stable with increasing model width. This is evident from the coordinate check plots for all the optimizers (Figs. 6 - 10 and Figs. 14 - 17). Under standard parameterization, the top row of the coordinate check plots shows that the relative mean of the feature vectors blow-up with increasing model width. With the incorporation of μP in the codebase, the relative mean values of the feature vectors stabilize with increasing model width (middle row of coordinate check plots).

It is interesting to note that since the theoretical underpinnings for μP hold in infinite width (Yang & Hu (2020)), the model width has to be "large enough" for the coordinate check plots to stabilize. This is especially observed in the coordinate check plots for LAMB (Fig. 9 and Fig. 16) where the mean values of the feature vectors initially increase, but gradually stabilize with increasing model width. This phenomenon is also observed in Fig. 2 which demonstrate the zero-shot learning rate transfer across model width on the NanoGPT model. In the minimum validation loss tables for ADOPT (Table 7) and LAMB (Table 11) the optimal value of the learning rate gradually stabilizes after a width of 256, whereas for AdamW (Table 5) and Sophia (Table 9) the optimal learning rate stabilizes after a width of 128. These inconsistencies across optimizers also suggest that introducing a "base model width" for μP scalings will introduce another HP. Therefore, we fix the value of the base model width to 1 in our implementation. In comparison to NanoGPT, the width scaling plots (Fig. 3) for Llama2 show that the model is "large enough" for the optimal learning rate to stabilize

from the smallest model width of 128. This is perhaps because for width of 128, the total number of parameters in Llama2 is significantly higher than the total number of parameters in NanoGPT.

The second set of simulations empirically evaluate the performance of the depth-scaling parameterization in existing works (Yang et al. (2023b); Dey et al. (2025)). The coordinate check plots (bottom row) for depth-scaling demonstrate that the feature vectors are stable with increasing model depth. In the coordinate check plots for ADOPT and LAMB (Figs. 7 and 9) the feature vectors stabilize after a depth of 16, while for AdamW, Sophia and Shampoo (Figs. 6, 8 and 10) the feature vectors are stable for shallow depths too. This phenomenon is similar to our observations for μP , because the depth-scaling parameterization is also derived for an infinite depth limit (Yang et al. (2023b)). Therefore, to prevent tuning an additional "base model depth" HP, we fix its value to 1 in our simulation setup. However, the loss plots in Figs. 11, 12 and 13 do not consistently demonstrate zero-shot learning rate transfer across increasing model depths. While the validation loss tables for AdamW (Table 6) and Sophia (Table 10) demonstrate that the optimal value of the learning rate stabilizes for deep models, the same is not observed for ADOPT (Table 8), LAMB (Table 12) and Shampoo (Table 14), where the value of the optimal learning rate oscillates as the depth is increased. These results suggest that deriving depth-scaling parameterization for different optimizers needs a more thorough theoretical analysis. Additionally, performing simulations on a finer grid of learning rates can also give further insights into the depth-scaling behavior.

B.2 μ P ON NANOGPT

Table 3: Hyperparameter values and training settings to test μP on NanoGPT model.

Architecture	NanoGPT Karpathy (2022)
Width	128 (scaled to 2048)
Depth	8
Number of heads	2
Total parameters	1.59 M (scaled to 403 M)
Dataset	Tiny Shakespeare
Vocab size	65
Tokens per iteration	8192
Batch size	2
Stopping criteria	Early stopping if validation loss doesnot improve in last 150 iterations
Optimizers	AdamW / ADOPT / LAMB / Sophia / Shampoo
Hyperparameter search range	$\eta \in [2 \times 10^{-1}, 2 \times 10^{-5}]$

Table 4: Hyperparameter values and training settings to test depth-scaling parameterization on NanoGPT model.

Architecture	NanoGPT Karpathy (2022)		
Width	256		
Depth	2 (scaled to 64)		
Total parameters	1.6 M (scaled to 50.56 M)		
Dataset	Tiny Shakespeare		
Vocab size	65		
Tokens per iteration	8192		
Batch size	2		
Stopping criteria	Early stopping if validation loss doesnot improve in last 150 iterations		
Optimizers	AdamW / ADOPT / LAMB / Sophia / Shampoo		
Hyperparameter search range	$\eta \in [2 \times 10^{-1}, 2 \times 10^{-5}]$		

B.2.1 ADAMW OPTIMIZER

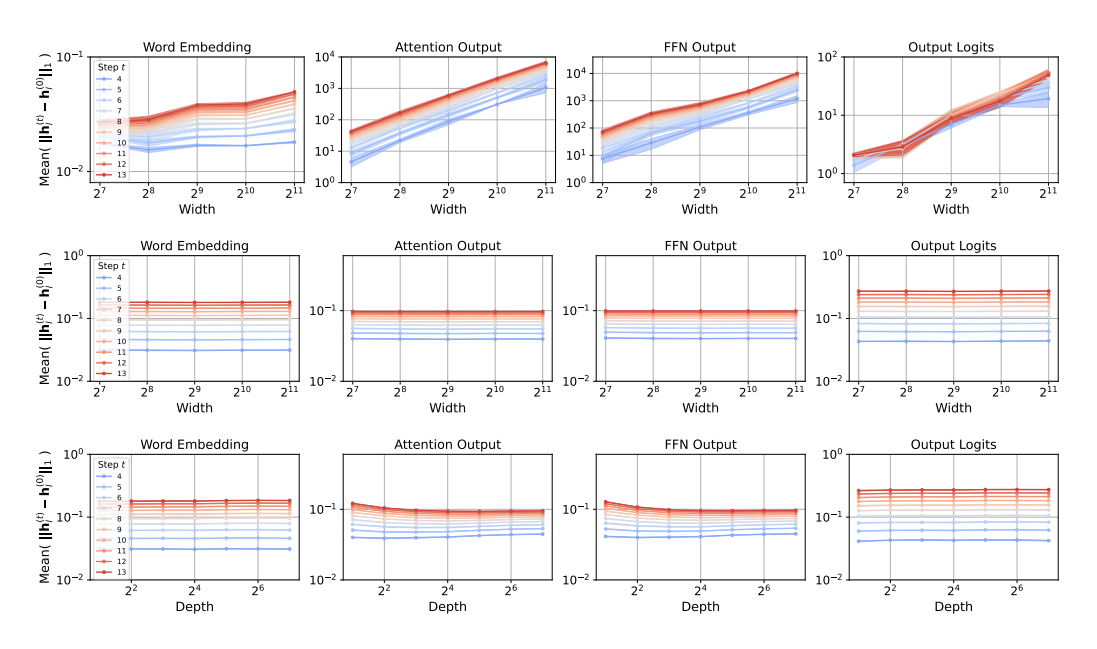


Figure 6: Coordinate check plots for AdamW under standard parameterization (top row), μ P (middle row); depth scaling (bottom row) for NanoGPT model.

Table 5: Mean validation loss for increasing model width and different learning rates for AdamW on NanoGPT model. The minimum loss for each width is highlighted in green.

LR / Width	128	256	512	1024	2048
2×10^{-1}	2.54111195	2.54770319	2.50132585	2.53559383	2.45719266
2×10^{-2}	2.57009896	2.56583707	2.57900651	2.53385917	2.51431378
2×10^{-3}	2.63474766	2.6022807	2.64679337	2.63449661	2.55710355
2×10^{-4}	3.38827054	3.5544157	3.38896998	3.44941664	3.44561863
2×10^{-5}	4.09221347	4.08871428	4.05257797	4.08837303	4.08405908

Table 6: Mean validation loss for increasing model depth and different learning rates for AdamW on NanoGPT model. The minimum loss for each depth is highlighted in green.

LR / Depth	2	4	8	16	32	64
2×10^{-1}	2.53525917	2.55192765	2.53510944	2.50357556	2.51294963	2.53008548
5×10^{-2}	2.52700798	2.49422677	2.50334986	2.29428236	2.45176029	2.36860998
2×10^{-2}	2.55682977	2.52176666	2.56583563	2.30422862	2.45500112	2.5650301
2×10^{-3}	2.59745781	2.63078475	2.60228316	2.61588136	2.64065663	2.65051214
2×10^{-4}	3.41396125	3.41677833	3.55441554	3.45801504	3.43285489	3.47577778
2×10^{-5}	4.09297959	4.05970796	4.08871428	4.08113146	4.06712834	4.10902596

B.2.2 ADOPT OPTIMIZER

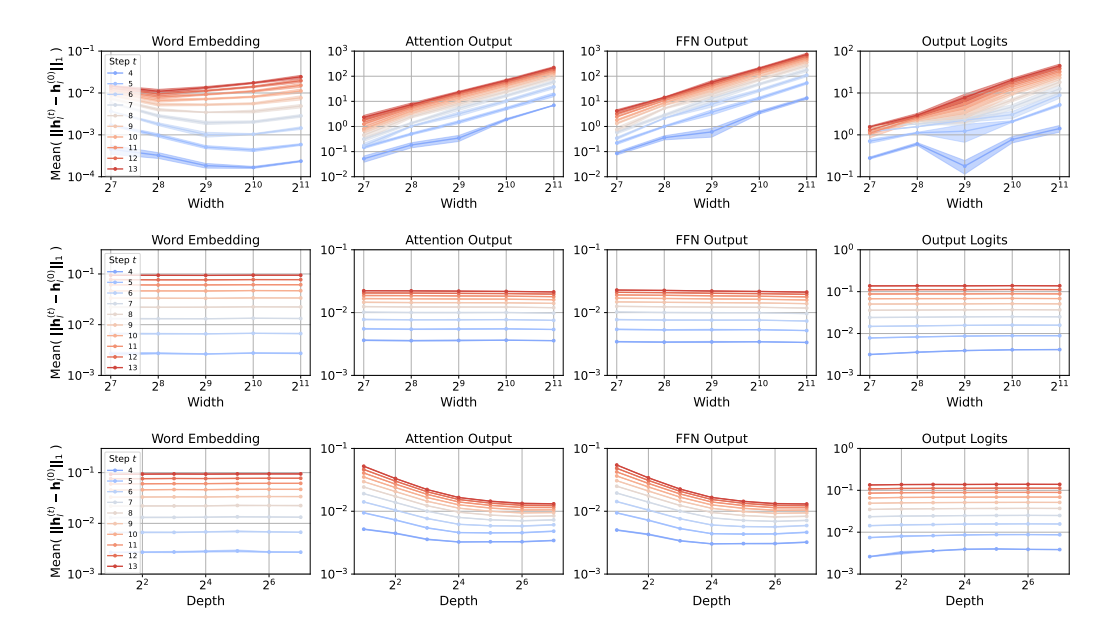


Figure 7: Coordinate check plots for ADOPT optimizer under SP (top row); μ P (middle row); depth scaling (bottom row) for NanoGPT model.

Table 7: Mean validation loss for increasing model width and different learning rates for ADOPT on NanoGPT model. The minimum loss for each width is highlighted in green.

LR / Width	128	256	512	1024	2048
2×10^{-1}	2.55120134	2.54616404	2.54178079	2.5524296	2.54457998
7×10^{-2}	2.48560476	2.44316975	2.37087123	2.50733534	2.50883015
2×10^{-2}	2.43175697	2.58847451	2.57006375	2.54323697	2.53191725
2×10^{-3}	2.63016931	2.6073552	2.65681744	2.66118956	2.55337548
2×10^{-4}	3.528404	3.49065232	3.49065232	3.42789133	3.43255997
2×10^{-5}	4.09183598	4.08832375	4.0521698	4.08806594	4.08391444

Table 8: Mean validation loss for increasing model depth and different learning rates for ADOPT on NanoGPT model. The minimum loss for each depth is highlighted in green.

LR / Depth	2	4	8	16	32	64
2×10^{-1}	2.56129368	2.51452438	2.54788987	2.51456078	2.52271922	2.55469418
9×10^{-2}	2.48695572	2.47477563	2.53124801	2.48145302	2.50687472	2.54724765
2×10^{-2}	2.56718413	2.50419029	2.58847276	2.44447954	2.54996069	2.52524622
2×10^{-3}	2.67992798	2.62949713	2.6073552	2.60433618	2.61753988	2.6286815
2×10^{-4}	3.41052596	3.46538957	3.56757394	3.47856442	3.43608022	3.56190586
2×10^{-5}	4.09267759	4.05929391	4.08832375	4.08074443	4.06675259	4.10877307

B.2.3 SOPHIA OPTIMIZER

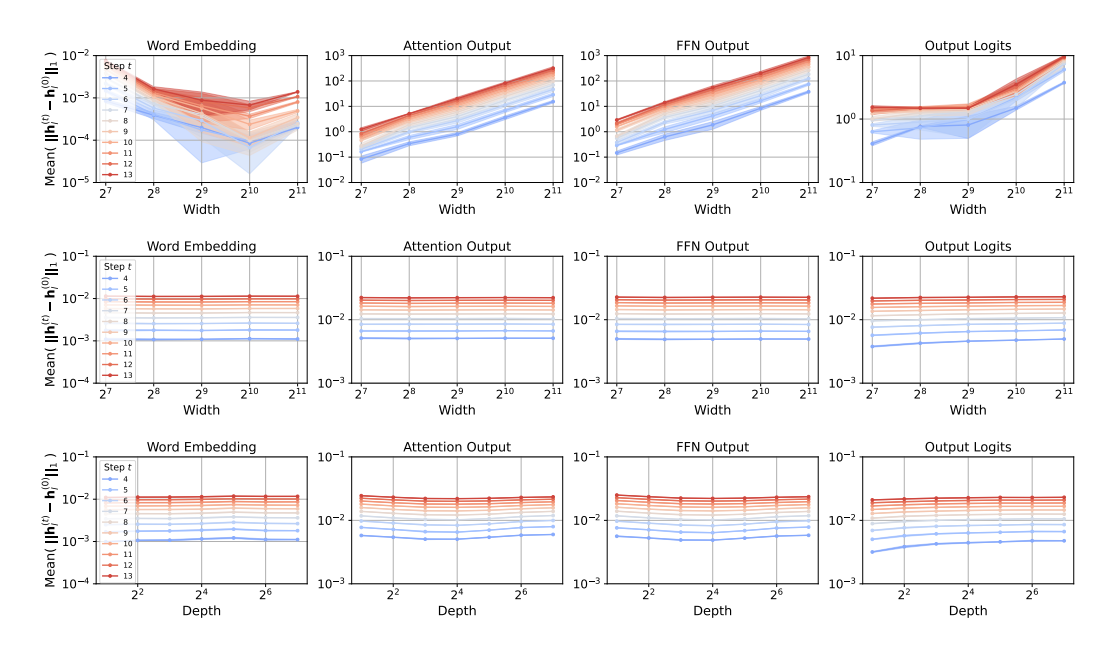


Figure 8: Coordinate check plots for Sophia optimizer under SP (top row); μ P (middle row); depth scaling (bottom row) for NanoGPT model.

Table 9: Mean validation loss for increasing model width and different learning rates for Sophia on NanoGPT model. The minimum loss for each width is highlighted in green.

LR / Width	128	256	512	1024	2048
2×10^{-1}	3.0969398	2.57144117	2.56875261	2.62573036	2.57240287
2×10^{-2}	2.27450609	2.27830847	2.31632638	2.53347905	1.98427689
2×10^{-3}	2.5456597	2.61430057	2.5594302	2.54869485	2.65462987
2×10^{-4}	3.35409013	3.54614369	3.36089802	3.35862382	3.36431138
2×10^{-5}	4.08766381	4.08859126	4.06069756	4.08811712	4.08371623

Table 10: Mean validation loss for increasing model depth and different learning rates for Sophia on NanoGPT model. The minimum loss for each depth is highlighted in green.

LR / Depth	2	4	8	16	32	64
2×10^{-1}	2.5213503	3.01081316	3.22649105	3.34855215	3.24310446	3.12229093
2×10^{-2}	2.4717048	2.27232289	2.24736114	2.47475751	2.46061246	1.93401444
2×10^{-3}	2.54103192	2.58136233	2.61035593	2.610612	2.45068415	2.55488427
2×10^{-4}	3.40887721	3.52765425	3.54587563	3.40669481	3.33997742	3.47574107
2×10^{-5}	4.09267314	4.06576761	4.08859126	4.08140405	4.066552	4.10874732

B.2.4 LAMB OPTIMIZER

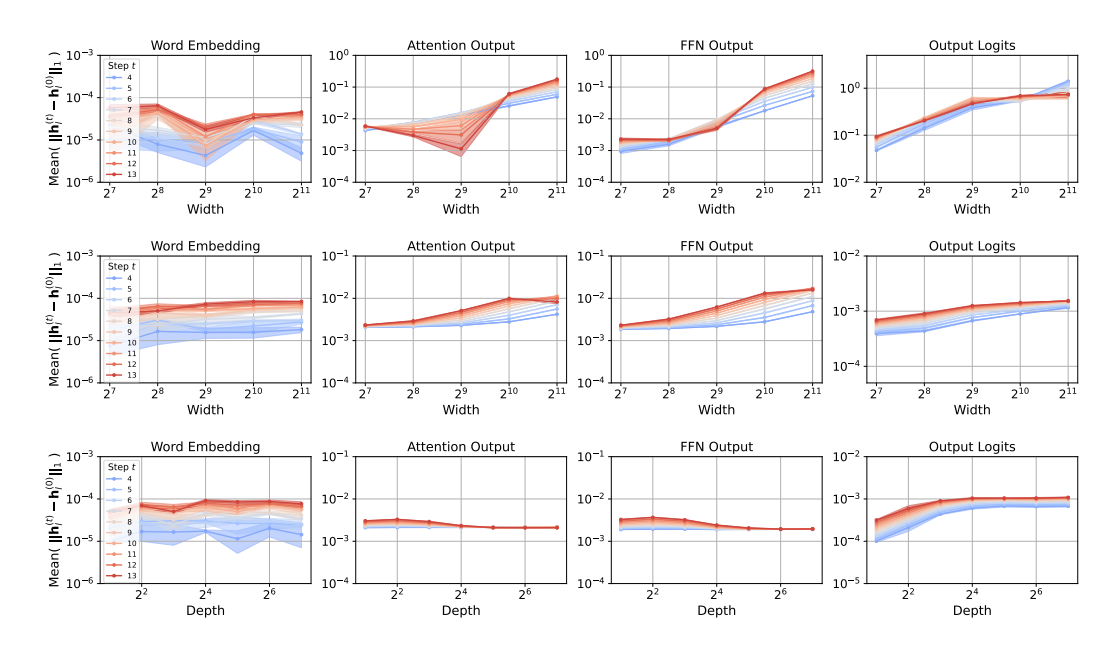


Figure 9: Coordinate check plots for LAMB optimizer under SP (top row); μ P (middle row); depth scaling (bottom row) for NanoGPT model.

Table 11: Mean validation loss for increasing model width and different learning rates for LAMB on NanoGPT model. The minimum loss for each width is highlighted in green.

LR / Width	128	256	512	1024	2048
2×10^{-1}	3.3306915	2.91992474	2.75658234	2.84724092	2.84511503
2×10^{-2}	2.27427769	2.55330944	2.53250345	2.50694895	2.51612274
2×10^{-3}	2.46762419	2.42723028	2.47571055	2.49152549	2.46575729
2×10^{-4}	3.69672974	3.70961714	3.66877778	3.2370429	3.37923479
2×10^{-5}	4.16929531	4.1694754	4.1684103	4.1674579	4.16771809

Table 12: Mean validation loss for increasing model depth and different learning rates for LAMB on NanoGPT model. The minimum loss for each depth is highlighted in green.

LR / Depth	2	4	8	16	32	64
2×10^{-1}	2.76534136	2.85949779	2.88115621	3.26932732	3.24093787	3.097018
2×10^{-2}	2.50858307	2.51164389	2.55355501	2.33967662	2.48308444	2.11406271
7×10^{-3}	2.45117172	2.46691815	2.50231234	2.45691435	2.48629936	2.45780365
2×10^{-3}	2.50483624	2.54284684	2.42723123	2.43291903	2.43262172	2.42000318
2×10^{-4}	3.6441706	3.79367606	3.70963343	3.57373738	3.61402575	3.42223287
2×10^{-5}	4.16981506	4.1691486	4.1694754	4.16932933	4.16817395	4.16773876

B.2.5 SHAMPOO OPTIMIZER

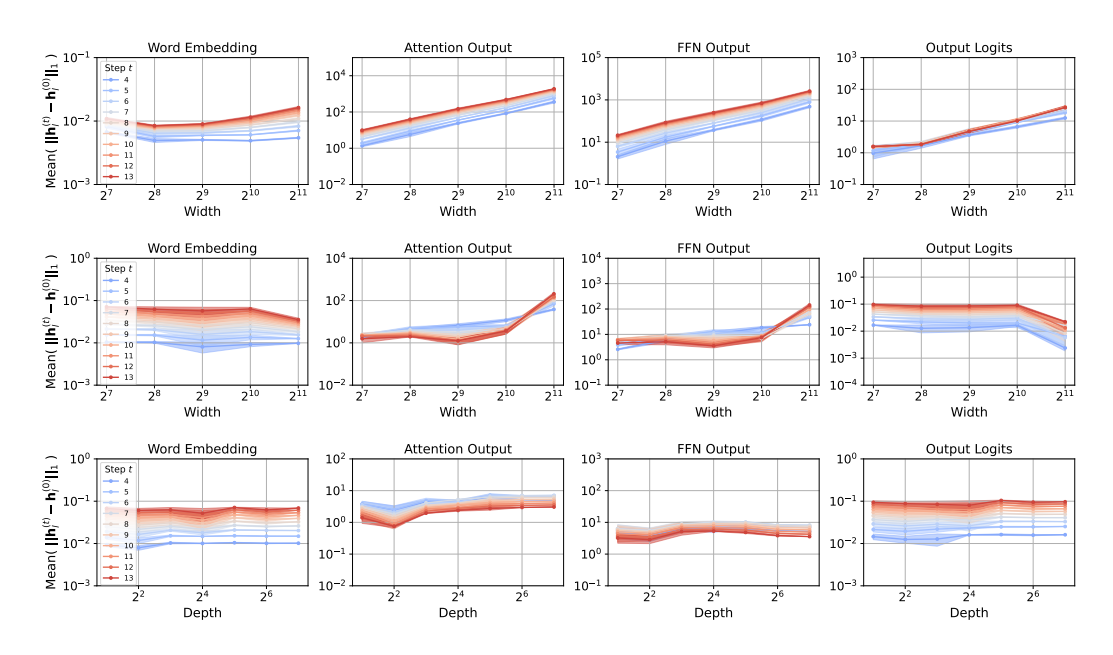


Figure 10: Coordinate check plots for Shampoo optimizer under SP (top row); μ P (middle row); depth scaling (bottom row) for NanoGPT model.

Table 13: Mean validation loss for increasing model width and different learning rates for Shampoo on NanoGPT model. The minimum loss for each width is highlighted in green.

LR / Width	128	256	512	1024	2048
1×10^{-2}	2.64432065	3.00841006	3.26729711	3.39512682	4.17380921
9×10^{-3}	2.6650331	2.89549454	3.20741065	3.45321918	3.41602135
5×10^{-3}	2.63122805	2.67693043	3.30215279	3.32265353	3.36052688
3×10^{-3}	2.67303157	2.85103401	3.37194387	3.46975843	3.49201838
1×10^{-3}	2.90583165	2.97975628	3.61035117	3.57224735	3.72281067

Table 14: Mean validation loss for increasing model depth and different learning rates for Shampoo on NanoGPT model. The minimum loss for each depth is highlighted in green.

LR / Depth	2	4	8	16	32	64
3×10^{-2}	2.83468819	2.94637481	3.3811605	3.27378623	3.32534583	3.31375853
1×10^{-2}	2.63917089	2.6383814	2.66823014	3.2278808	3.24864435	3.20088768
7×10^{-3}	2.64190022	2.61007253	2.73991227	3.12863938	3.20985778	3.37485345
5×10^{-3}	2.77703945	2.72295157	2.72794461	2.93629122	3.25431808	3.37258538
3×10^{-3}	2.7143542	2.97368789	2.85365486	3.32030662	3.27988537	3.40830247

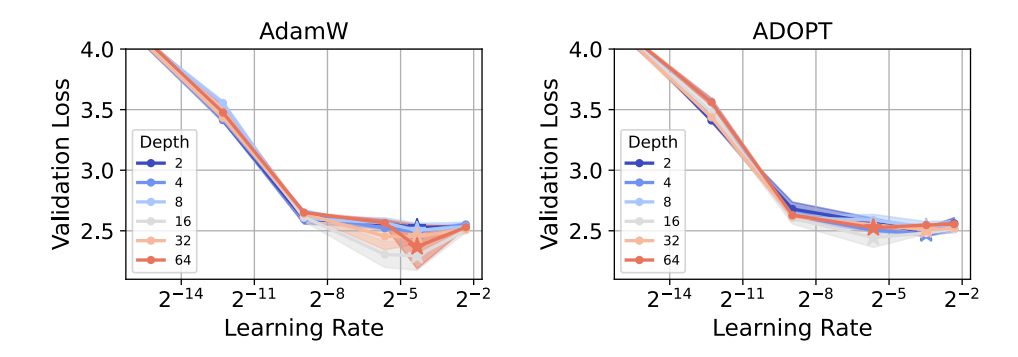


Figure 11: Mean validation loss for increasing model depth and different learning rates for AdamW (left) and ADOPT (right) on NanoGPT model.

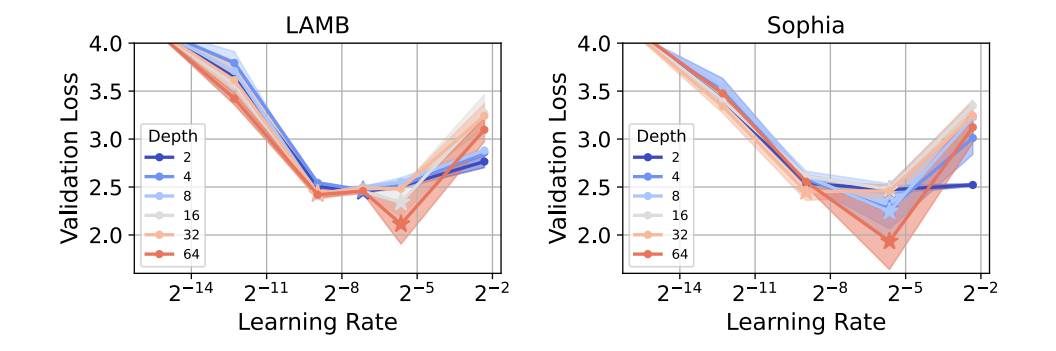


Figure 12: Mean validation loss for increasing model depth and different learning rates for LAMB (left) and Sophia (right) on NanoGPT model.

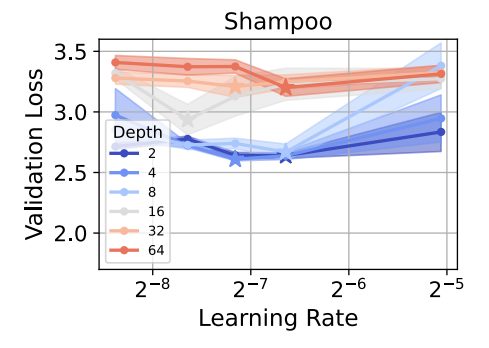


Figure 13: Mean validation loss for increasing model depth and different learning rates for Shampoo on NanoGPT model.

B.3 μ P on Llama2

Table 15: Hyperparameter values and training settings to test μP on Llama2 model.

Architecture	Llama 2		
Width	256 (scaled to 2048)		
Depth	16		
Number of attention heads	32		
Total parameters	154M (scaled to 1.38 B)		
Dataset	Wikitext-103		
Sequence length	4096		
Vocab size	32000		
Training set tokens	100M		
Batch size	192		
Training steps	1026		
LR decay style	cosine rule, 51 steps warm-up		
Optimizer	AdamW / ADOPT / LAMB / Sophi		
Weight decay	0.1		
Dropout	0.0		
μP HP search range	$\eta \in [5 \times 10^{-1}, 5 \times 10^{-4}]$		

B.3.1 ADAMW

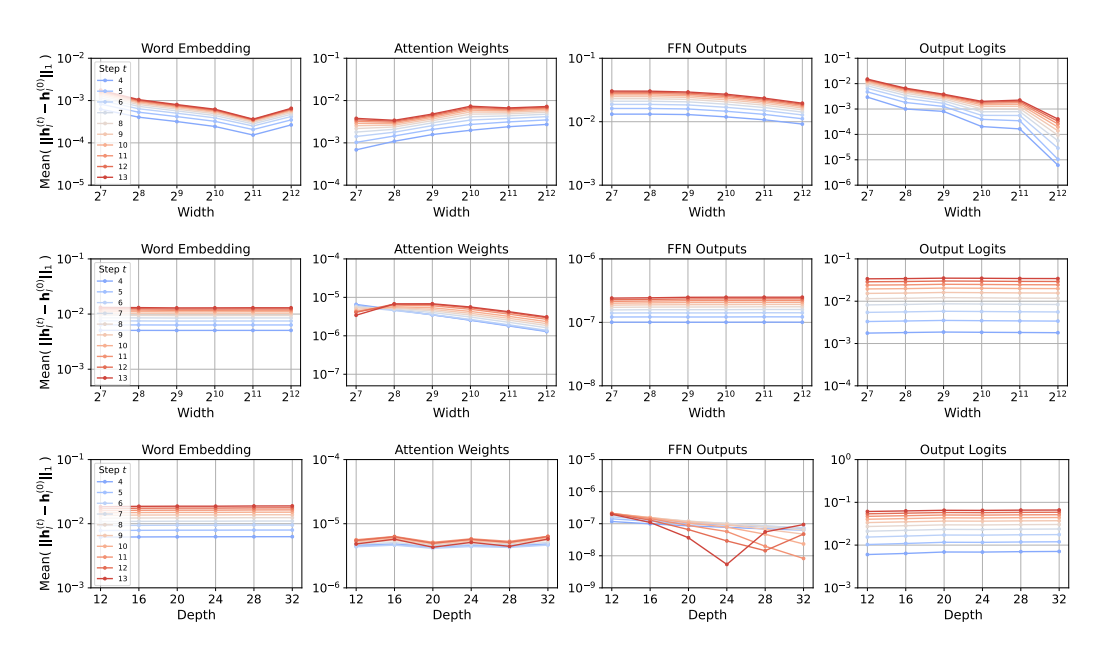


Figure 14: Coordinate check plots for AdamW optimizer under SP (top row); μ P (middle row); depth scaling (bottom row) for Llama2 model.

Table 16: Validation loss for increasing model width and different learning rates for AdamW on Llama2 model. The minimum loss for each width is highlighted in green.

LR / Width	128	256	512	1024	2048
5×10^{-1}	4.55491	4.02676	3.81251	3.73573	3.79477
3×10^{-1}	4.24978	3.90242	3.83252	3.89484	3.75046
1×10^{-1}	4.48696	4.21314	4.05265	4.02101	3.95419
5×10^{-2}	4.70421	4.4353	4.39753	4.34169	4.31635
1×10^{-1}	5.57795	5.56284	5.56173	5.55771	5.55774

B.3.2 ADOPT

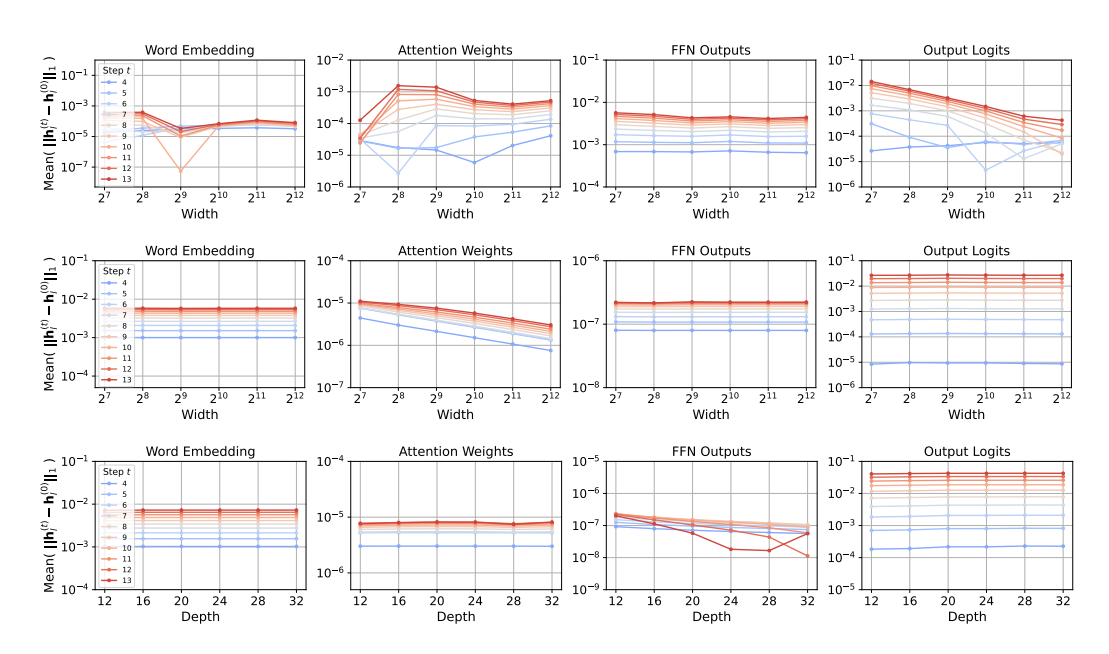


Figure 15: Coordinate check plots for ADOPT optimizer under SP (top row); μ P (middle row); depth scaling (bottom row) for Llama2 model.

Table 17: Validation loss for increasing model width and different learning rates for ADOPT on Llama2 model. The minimum loss for each width is highlighted in green.

LR / Width	128	256	512	1024	2048
5×10^{-1}	4.39033	4.02007	3.83932	3.77732	3.76814
3×10^{-1}	4.11789	3.85536	3.72552	3.67802	3.66973
2×10^{-1}	4.23765	3.87949	3.78242	3.80016	3.78846
1×10^{-1}	4.32335	4.07597	3.9912	3.91654	3.95519
7×10^{-2}	4.43819	4.22574	4.13565	4.06852	4.0683
5×10^{-2}	4.64121	4.38096	4.31582	4.22186	4.21248

B.3.3 LAMB

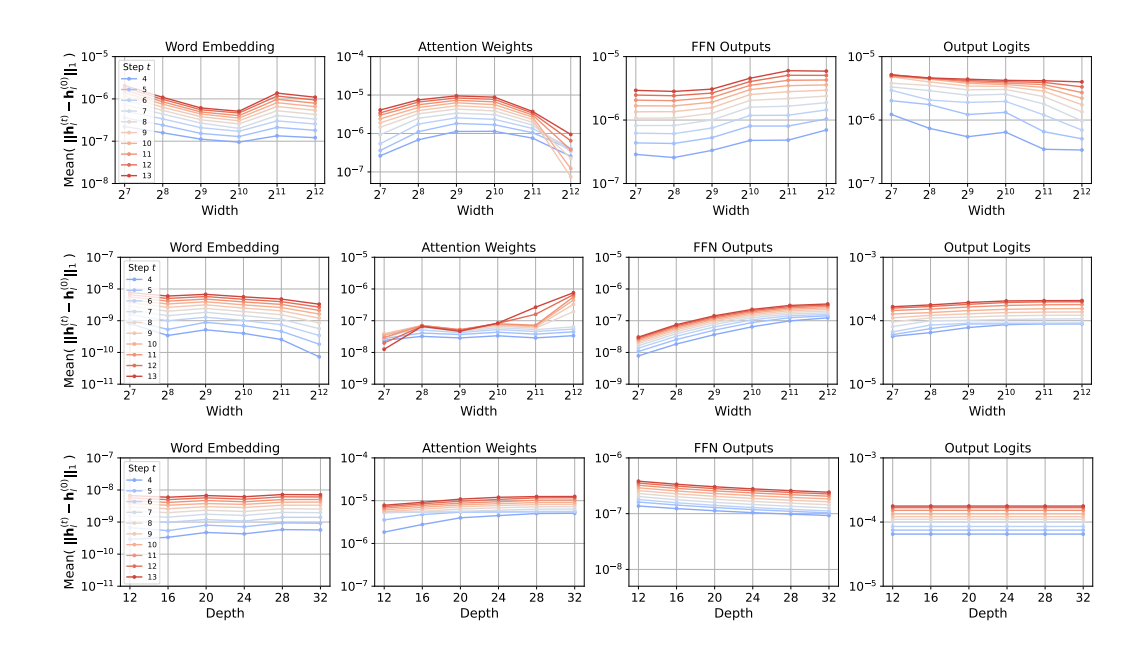


Figure 16: Coordinate check plots for LAMB optimizer under SP (top row); μ P (middle row); depth scaling (bottom row) for Llama2 model.

Table 18: Validation loss for increasing model width and different learning rates for LAMB on Llama2 model. The minimum loss for each width is highlighted in green.

LR / Width	128	256	512	1024	2048
3×10^{-2}	7.18452	6.35059	6.0384	6.52966	6.13429
1×10^{-2}	5.58878	5.5638	5.56049	5.79174	6.01439
5×10^{-3}	6.57476	6.60454	6.66398	6.98093	7.0471
1×10^{-3}	10.25112	10.23998	10.22575	10.21199	10.19599
5×10^{-4}	10.32997	10.32776	10.32398	10.32062	10.31677

B.3.4 SOPHIA

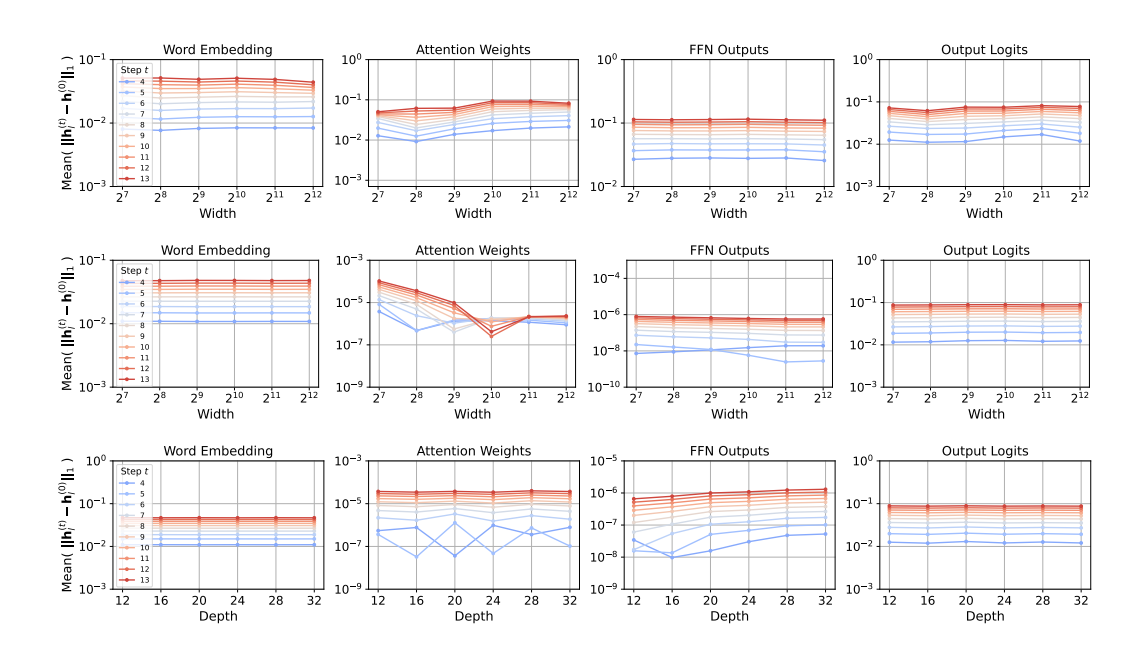


Figure 17: Coordinate check plots for Sophia optimizer under SP (top row); μ P (middle row); depth scaling (bottom row) for Llama2 model.

Table 19: Validation loss for increasing model width and different learning rates for Sophia on Llama2 model. The minimum loss for each width is highlighted in green.

LR / Width	128	256	512	1024	2048
5×10^{-1}	7.19403	6.99576	6.68992	6.60376	6.31375
3×10^{-1}	6.17604	5.90826	5.80694	5.6738	5.71962
1×10^{-1}	4.14122	3.83654	3.75926	3.67419	3.62891
7×10^{-2}	4.42758	4.31702	4.05756	3.93561	3.94189
5×10^{-2}	4.76632	4.51022	4.41358	4.34452	4.30914
3×10^{-2}	4.82305	4.79592	4.73067	4.67473	4.74689